



EDGEWOOD

CHEMICAL BIOLOGICAL CENTER

U.S. ARMY RESEARCH, DEVELOPMENT AND ENGINEERING COMMAND

ECBC-TR-636

CONFORMATIONAL CHANGES IN SMALL LIGANDS UPON TETANUS TOXIN BINDING

Terry J. Henderson

RESEARCH AND TECHNOLOGY DIRECTORATE

Rossitza K. Gitti



SCIENCE APPLICATIONS
INTERNATIONAL CORPORATION
Abingdon, MD 21009

June 2008

Approved for public release;
distribution is unlimited.



20080911260

ABERDEEN PROVING GROUND, MD 21010-5424

Disclaimer

The findings in this report are not to be construed as an official Department of the Army position unless so designated by other authorizing documents.

Blank

PREFACE

The work described in this report was authorized under Project No. 8EA1DB. The work was started in April 2006 and completed in May 2008.

The use of either trade or manufacturers' names in this report does not constitute an official endorsement of any commercial products. This report may not be cited for purposes of advertisement.

This report has been approved for public release. Registered users should request additional copies from the Defense Technical Information Center; unregistered users should direct such requests to the National Technical Information Service.

Acknowledgments

The authors would like to acknowledge the Research and Technology Directorate In-House Laboratory Independent Research (ILIR) Committee for funding this work.

Blank

CONTENTS

| | | |
|-------|---|----|
| 1. | INTRODUCTION | 7 |
| 2. | EXPERIMENTAL PROCEDURES | 10 |
| 2.1 | Recombinant Proteins, Ligands, Solvents, and Supplies | 10 |
| 2.2 | Preparation of Ligand and TetC-Ligand Samples | 10 |
| 2.3 | NMR Instrumentation and Spectroscopy | 11 |
| 2.3.1 | One-Dimensional Spectroscopy and Relaxation Time Measurements | 12 |
| 2.3.2 | COSY and HSQC Spectroscopy | 12 |
| 2.3.3 | NOESY and trNOESY | 13 |
| 3. | RESULTS AND DISCUSSION | 13 |
| 3.1 | Assignment of Ligand ^1H and ^{13}C Signals | 13 |
| 3.2 | NMR Relaxation and Conformational Flexibility | 14 |
| 3.3 | NOESY and trNOESY Analysis | 15 |
| 4. | CONCLUSIONS | 18 |
| | LITERATURE CITED | 21 |

FIGURES

| | | |
|----|--|----|
| 1. | Doxorubicin and Lavendustin A..... | 8 |
| 2. | Crystal Structure of TetC Determined to 1.6 Å Resolution..... | 9 |
| 3. | Aromatic Regions of the Doxorubicin and Lavendustin A NOESY Spectra with the Doxorubicin-TetC-lavendustin A Complex trNOESY Spectrum..... | 16 |
| 4. | Superposition of the Aromatic Regions from the Doxorubicin NOESY Spectrum and TrNOESY Spectrum..... | 17 |
| 5. | Doxorubicin Bound to TetC..... | 18 |
| 6. | Lavendustin A Bound to the TetC Fragment..... | 18 |

TABLES

| | | |
|----|--|----|
| 1. | Summary of NOESY and trNOESY Samples | 11 |
| 2. | ^{13}C and ^1H Chemical Shift Values for Doxorubicin in D_2O | 13 |
| 3. | 125.77 MHz $^{13}\text{C}\{^1\text{H}\}$ T_1 and NT_1 Values for Doxorubicin | 15 |

CONFORMATIONAL CHANGES IN SMALL LIGANDS UPON TETANUS TOXIN BINDING

1. INTRODUCTION

Recent biological attacks involving the ricin toxin have highlighted the need for a fast and reliable method for detecting bioterrorism agents. Tests for these toxins typically rely upon established biochemical methods, such as enzyme-linked immunosorbant assays (ELISA), and require a detection molecule that offers specific recognition to the target toxins. Antibodies have traditionally been used as the detection molecules for these methods. Today, automated detection methods are being developed for the continuous monitoring of high-risk areas such as airports, post offices, and government buildings. Recognition molecules for these devices must not only be sensitive and specific but also robust and capable of monitoring complex environmental samples over extended periods of time without significant loss of activity. Because of their absolute requirement of a complex, rigid conformation (three-dimensional structure) for binding activity, a conformation that can be easily compromised outside of physiological conditions, antibodies are not well suited for use as detection molecules in such devices. There are an ever-increasing number of laboratories investigating the use of small molecules towards these ends. Several recent studies, for example, have demonstrated that glycosphingolipids can be used for the sensitive and reliable recognition of certain protein toxins, including ricin, botulinum, tetanus toxin and cholera toxin.¹⁻⁶ Small molecules offer several potential advantages over antibodies, including increased stability under ambient conditions, ease of orientation at the detector surface, and a large number of binding sites per unit area compared to larger antibody molecules.

An alternative approach for designing small molecule detectors is to identify a number of such molecules that bind the surface of a protein toxin and link two or more together in a manner to produce a multidentate, synthetic, high-affinity ligand with a very high specificity for the toxin target. Recent developments in computer modeling and computational methods for screening an enormously large number of small molecule structures for their ability to bind the surface of a protein target⁷ facilitates the process tremendously, allowing such an approach to be manageable for the first time. Largely because of their size, the individual small molecules identified by these screening procedures usually bind only weakly the protein target. However, the free energy of binding for a multidentate ligand constructed from them is, in principle, the sum of the free energies of each small molecule alone plus a term owing to linking the small molecules.⁸ Linked compounds with less than micromolar dissociation constants can be obtained by linking two or more small molecules that each dissociate in the greater than micromolar range.⁹ The binding affinity and specificity of the resulting ligand can be engineered to a large degree simply by selecting different small molecules to bind at least two sites on the protein toxin's surface.

By using extensive computer modeling along with spectroscopic methods, Balhorn and co-workers¹⁰⁻¹¹ recently have identified nine different small molecules that bind the tetanus toxin (TeNT) surface. One of these compounds, doxorubicin, was found to have strong hydrophobic interactions with the toxin surface and was measured to have a 9.4 μM binding constant.¹¹ Lavendustin A was found to bind the TeNT surface at a different site in a manner

that does not compromise TeNT-doxorubicin binding.¹⁰ The two molecules represent very good candidates for use in the rational design of a bidentate ligand binds with high specificity and affinity to TeNT. The chemical structures of doxorubicin and lavendustin A are shown in Figure 1 together with a numbering scheme for doxorubicin carbon atom sites.¹²

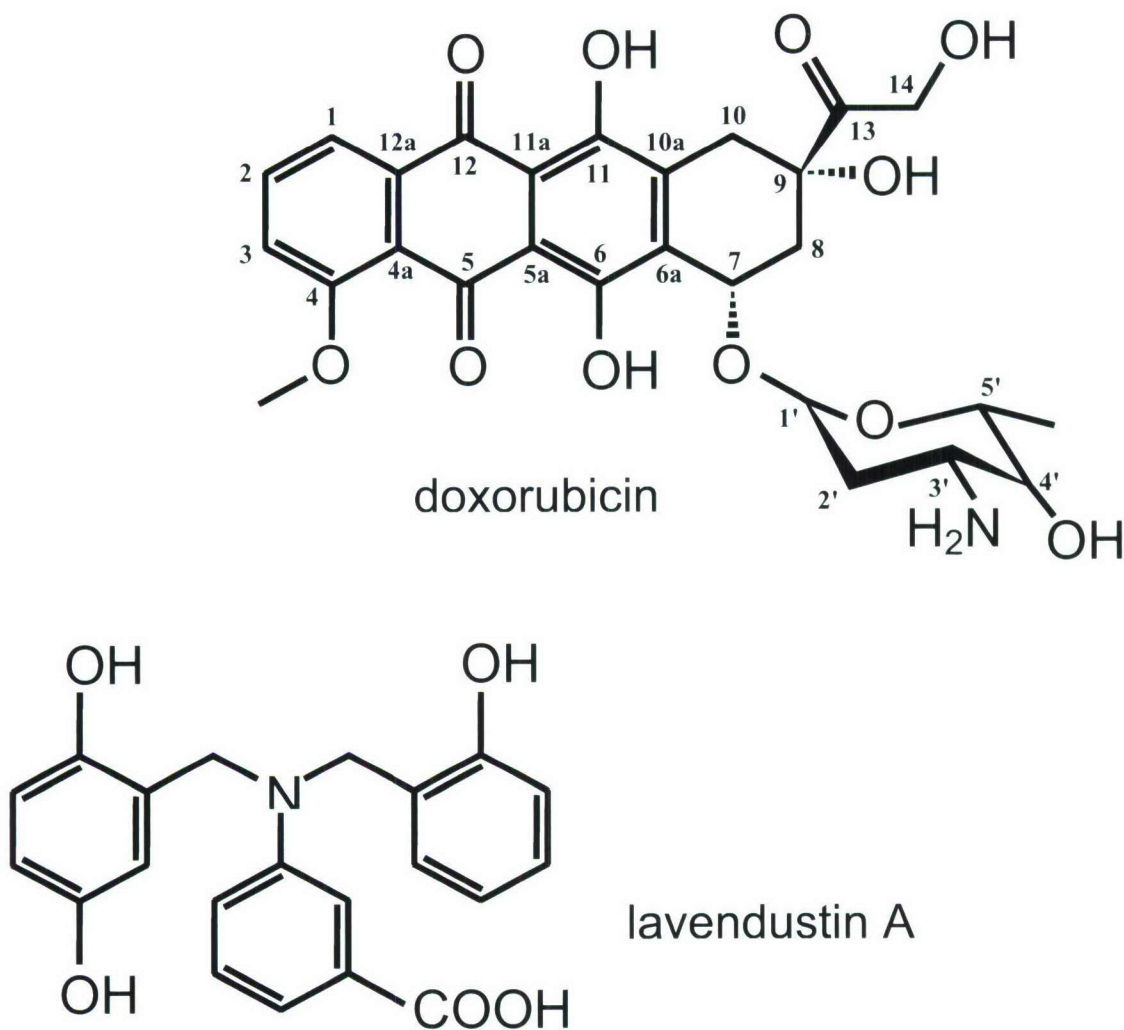


Figure 1. Doxorubicin and Lavendustin A. Numbers refer to the individual doxorubicin carbon atom sites and are adopted from the numbering scheme presented by Searle and co-workers.¹²

TeNT and the seven serotypes of botulinum toxin are structurally and functionally related members of the family of clostridial neurotoxins. The toxins all selectively concentrate at the synapse of axons in vertebrate motor neurons and are the most potent toxins known to man. TeNT specifically targets inhibitory neurons within the central nervous system and spinal cord to cause a spastic paralysis, while botulinum toxins target peripheral sensory neurons resulting in flaccid paralysis. Both toxins are synthesized as single 150 kDa polypeptides that are subsequently processed into two chains held together by a single disulfide bond. Although the mechanism by which the toxins enter living cells is not fully understood, gangliosides have a

high selective affinity for these neurotoxins, and it is believed that the initial step must involve the binding of the toxin to gangliosides located on the surface of the cell.¹³ TeNT has been shown specifically to bind gangliosides of the G1b series, GD1b or GT1b.¹⁴⁻¹⁷ The receptor binding subunit of TeNT is a 51 kDa polypeptide containing the C-terminal 452 amino acids of the heavy chain, more commonly referred to as the C fragment.^{18,19} The last 34 amino acids of the TeNT C fragment (TetC, amino acid residues 875-1,315) are intimately involved in ganglioside recognition, with His1,293 absolutely critical for binding.^{19,20} Two TetC crystal structures show the toxin fragment to consist of two sub-domains, a lentil lectin-like N-terminal jelly-roll domain and a C-terminal β -trefoil domain;²¹ see Figure 2. The ganglioside binding site has been found to occur along one edge of the C-terminal β -trefoil sub-domain.²¹ The site is a common surface feature of the tetanus and botulinum toxins, and recent studies reveal that doxorubicin binds this site as well.^{10,22} Lavendustin A binds a second site on TetC, which occurs as a deep surface pocket located between the C-terminal β -trefoil and N-terminal jelly-roll sub-domains.¹⁰ The site has been identified as the most highly conserved pocket in the structures of the TeNT and botulinum toxins.²³

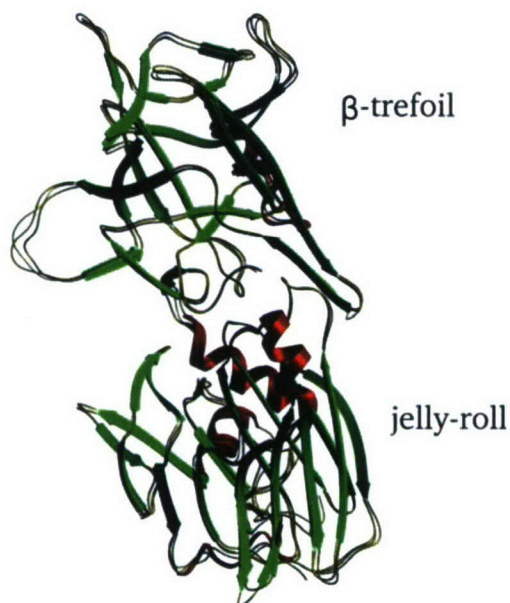


Figure 2: Crystal Structure of TetC Determined to 1.6 Å Resolution. α -Helices are red, β -sheets are green, and loop regions are displayed as black strings.

This effort is a preliminary investigation of the processes associated with small synthetic ligands binding to large protein surfaces. Nuclear magnetic resonance (NMR) spectroscopy was used together with computer molecular modeling to examine the conformational changes in doxorubicin and lavendustin A associated with their binding to TetC. ¹³C NMR spin-lattice relaxation times (T_1) were measured for specific carbon atom sites of the doxorubicin molecule for a detailed evaluation the conformational behavior of the ligand in solution. Additional conformational information was derived from nuclear Overhauser effect (NOE) enhancements measured for both ligands in solution by using conventional NOE spectroscopy (NOESY). Finally, the TetC-bound conformation for each ligand was inferred

from ^1H - ^1H distance constraints derived from transferred NOESY (trNOESY) data and comparison to the NOESY data.

2 EXPERIMENTAL PROCEDURES

2.1 Recombinant Proteins, Ligands, Solvents, and Supplies

A recombinant form of the tetanus toxin C fragment was purchased from Roche Diagnostics (Indianapolis, IN). Doxorubicin hydrobromide and crystalline lavendustin A were purchased from Sigma-Aldrich (St. Louis, MO) for use as ligands. The sodium salt of 3-(trimethylsilyl)-1-propane sulfonic acid was also purchased from Sigma-Aldrich for use as a chemical shift reference. D_2O and deuterated dimethyl- d_6 sulfoxide (DMSO), both >99.5% isotope enrichment, were purchased from Isotech, Inc. (Miamisburg, OH). All NMR sample tubes (Product number 535-PP-8) were purchased from Wilmad-Labglass (Buena, NJ).

Caution: The ligands used in this study are hazardous and should be handled carefully. The antitumor drug doxorubicin is an inhibitor of reverse transcriptase and RNA polymerase, is an immunosuppressive agent, and intercalates into DNA.²⁴⁻²⁶ Lavendustin A is a protein tyrosine kinase inhibitor.²⁷

2.2 Preparation of Ligand and TetC-Ligand Samples

In trNOESY experiments, the detection of intra-ligand ^1H - ^1H correlations, when bound to macromolecules, is intimately related to the ligand concentration and macromolecule-ligand molar ratio. Optimizing experimental conditions often includes evaluating a large number of samples, each with different ligand and macromolecule concentrations, at various experimental temperatures. Stock ligand solutions were prepared to simplify and facilitate the production of large numbers of trNOESY samples (containing one or two ligands and TetC), as well as NOESY samples (containing ligand only). Doxorubicin stock solutions were prepared by dissolving 4.2 mg of doxorubicin hydrobromide in 500 μL of D_2O . Lavendustin A stock solutions were prepared in deuterated DMSO because the ligand is only moderately soluble in water; 3.8 mg of crystalline lavendustin A was dissolved in 500 μL of the solvent. The stock solutions were typically stored at 4-8 $^\circ\text{C}$ for ≤ 6 months without detectable signs of degradation.

The sample yielding the highest trNOESY sensitivity for doxorubicin ^1H - ^1H correlations when bound to TetC was prepared by first dissolving 2.8 mg of lyophilized TetC in 1.0 mL of D_2O . The solution was centrifuged for 10 min in an Eppendorf microcentrifuge (Eppendorf AG, Hamburg, Germany) to remove insoluble material, and 740 μL of the resulting supernatant was collected and combined with 60 μL of the doxorubicin stock solution to produce the final sample. The analogous NOESY sample was prepared by simply adding 60 μL of the doxorubicin stock solution to 740 μL of D_2O . Additionally, 600 μL of a 10 mg/mL doxorubicin sample in D_2O was prepared for ^{13}C relaxation time measurements.

The sample giving the highest trNOESY sensitivity for lavendustin A ^1H - ^1H correlations when bound to TetC was prepared by first dissolving 2.2 mg of TetC in 1.0 mL of

D₂O and centrifuging as above. A 40 μ L aliquot of the lavendustin A stock solution was combined with 760 μ L of the resulting supernatant to give the final sample. An analogous NOESY sample was prepared by simply adding 40 μ L of the lavendustin A stock solution to 760 μ L of D₂O. As previously demonstrated by others,⁹ the small amount of DMSO would not be expected to denature the TetC protein. This was corroborated by the absence of precipitated material in the samples even 6 months after their preparation.

Finally, a doxorubicin-TetC-lavendustin A sample was prepared for trNOESY competition assays. For this sample, 2.9 mg of TetC was dissolved in 1.0 mL of D₂O, and after centrifugation of the resulting solution, 60 μ L of the doxorubicin stock solution and 40 μ L of the lavendustin A stock solution were added to 700 μ L of the supernatant to generate the final sample. All ligand and TetC concentrations for the NOESY and trNOESY samples, as well as their ligand-TetC molar ratios, are outlined in Table 1.

Table 1. Summary of NOESY and trNOESY Samples

| sample | Concentration (μM) | | TetC | TetC:Ligand Molar Ratio | |
|------------------------|--------------------|---------------|------|-------------------------|---------------|
| | doxorubicin | lavendustin A | | doxorubicin | lavendustin A |
| <i>NOESY Samples</i> | | | | | |
| 1 | 1081.4 | ----- | ---- | ---- | ---- |
| 2 | ----- | 993.3 | ---- | ---- | ---- |
| <i>trNOESY Samples</i> | | | | | |
| 3 | 1081.4 | ----- | 54.3 | 1:20 | ---- |
| 4 | ----- | 993.3 | 45.0 | ---- | 1:22 |
| 5 | 1081.4 | 993.3 | 54.0 | 1:20 | 1:18 |

2.3 NMR Instrumentation and Spectroscopy

All NMR spectroscopy was conducted at 11.75 Tesla, using an Avance DRX-500 spectrometer (Bruker-Biospin Corporation, Billerica, MA) with XWIN-NMR software (version 3.6) for data acquisition and processing. The spectrometer was fitted with a TCI probehead containing cryogenic ¹H and ¹³C channels, a conventional ¹⁵N channel, and an actively shielded z-gradient coil. A three-channel, 10-ampere Acustar II 3x10 gradient amplifier (Bruker-Biospin Corporation) was used to amplify gradient coil pulses, with all pulse timing controlled from the spectrometer pulse programs. Experiments were conducted at 20.0 \pm 0.2 or 25.0 \pm 0.2 $^{\circ}$ C, with the sample spinning at 20 Hz for one-dimensional experiments only. For two-dimensional spectroscopy, quadrature was used exclusively for collecting complex data in the direct dimension (t_2), while different phase cycling schemes used for the indirect dimension (t_1) to generate complex data. All ¹H decoupling used the WALTZ-16 composite pulse sequence,²⁸ and chemical shifts for ¹H and ¹³C spectra were referenced to external 3-(trimethylsilyl)-1-propane-sulfonic acid.

2.3.1 One-Dimensional Spectroscopy and Relaxation Time Measurements

Conventional ^1H free induction decay (FID) data of 16,384 complex points were summations of 32 acquisitions recorded with 10-12 ppm spectral windows, 90° pulse widths, and 5-9 sec relaxation delays. These were Fourier transformed directly into spectra and manually phase-corrected into pure absorption mode. For conventional $^{13}\text{C}\{^1\text{H}\}$ spectra, free FID data of 65,536 complex points and 8,192 acquisitions were recorded using 220 ppm spectral windows and 20 sec relaxation delays. Data were collected with 90° pulse widths, or alternatively, quantitative $^{13}\text{C}\{^1\text{H}\}$ data sets were recorded with the sensitivity-enhanced Q-DEPT pulse sequence.²⁹ Recorded data were multiplied by an exponential window function with a line-broadening factor of 2 Hz before Fourier transformation into spectra and manual phase correction into pure absorption mode.

For the measurement of doxorubicin NMR relaxation times, natural abundance $^{13}\text{C}\{^1\text{H}\}$ NMR experiments were conducted on a nonspinning sample at $25.0 \pm 0.2^\circ\text{C}$. T_1 measurements were based on the inversion recovery pulse sequence²⁹ [$180^\circ - \tau - 90^\circ$ - acquisition] with 8 randomized τ delays. Data sets from the accumulation of 65,536 complex points and 200 ppm spectral windows were obtained from the summation of 5,000 FID signals, with relaxation delays of at least five times the longest protonated ^{13}C T_1 value. FID data sets were apodized with a line broadening factor of 5 Hz before Fourier transformation into spectra and phase correction into pure adsorption mode. T_1 values were derived from fitting spectral signal intensities as a function of τ to single-exponential expressions.³⁰

2.3.2 COSY and HSQC Spectroscopy

^1H - ^1H correlation spectroscopy (COSY) was used to assign ^1H signals to specific protons of doxorubicin. In particular, scalar-coupled proton pairs were identified with a COSY pulse sequence using a pulsed-field gradient, double-quantum filter. Quadrature was achieved in the indirect dimension by using a time proportional phase incrementation (TPPI) phase cycling scheme³¹ to collect data sets contained 4,096 free induction decays, each with 8,192 complex points from two data accumulations using 1 sec relaxation delays to give a final 4,096 real X 8,192 complex ($t_1 \times t_2$) data matrix. Spectral windows of 6.4 ppm were used in both dimensions. The t_2 FID data were zero-filled to 16,384 complex points, then apodized with a line-broadening factor of 0.5 Hz before Fourier transformation. The resulting t_1 free FID data were zero-filled to 8,192 real points, apodized with a 1.5 Hz line-broadening factor, and finally Fourier transformed into a spectrum of 8,192 X 8,192 ($f_1 \times f_2$) real points.

Protons were correlated to their directly bonded carbon nuclei to facilitate the assignment of ^1H and ^{13}C signals of doxorubicin and lavendustin A to their respective nuclei. One-bond, ^1H - ^{13}C correlations were determined with a HSQC pulse sequence using an echo/antiecho-TPPI gradient scheme.³²⁻³⁴ A 1,024 X 8,192 complex data matrix was collected with 64 ^1H acquisitions per t_1 increment using 2 sec relaxation delays. The spectral widths used were 6.4 ppm in the ^1H dimension and 220 ppm for the indirect, ^{13}C dimension. ^1H data were apodized with a 4 Hz line-broadening factor before Fourier transformation. For t_1 , data points were extended to 4,096 complex points by linear prediction before multiplication with a sine-squared window function and final Fourier transformation into a 2,048 X 4,096 real spectrum.

2.3.3 NOESY and trNOESY

NOESY data sets were recorded with a pulse program incorporating gradient pulses during the mixing time³⁵ and quadrature in the indirect dimension by using a States-TPPI scheme.³⁶ Experiments with ligands in the absence of TetC were conducted with 900 msec mixing times, while those with ligands in the presence of TetC were conducted with 200 or 300 msec mixing times. Long mixing times are necessary for the detection of NOEs for molecules <1-2 kDa because the product of ω_0 ($2\pi \times$ spectrometer operating frequency) and τ_C (rotational correlation time) is < 1 ($\omega_0\tau_C < 1$); in contrast, shorter mixing times are required for larger molecules or small molecule ligands binding to macromolecules because $\omega_0\tau_C \gg 1$.³⁷ Data sets were collected as a 300 x 1,024 complex matrix using 7.0 ppm spectral windows in both dimensions. Each t_2 FID resulted from 64 acquisitions with 2 sec relaxation delays. The t_2 data were multiplied by a sine window function before Fourier transformation. The resulting FID data were extended to 600 complex points with a linear prediction algorithm,^{38,39} multiplied by a sine window function, and finally Fourier transformed into a 600 x 512 real spectrum.

3 RESULTS AND DISCUSSION

3.1 Assignment of Ligand ^1H and ^{13}C Signals

The NMR signal for each ^1H and ^{13}C atomic site of doxorubicin was unambiguously identified by using routine NMR spectroscopy along with COSY and HSQC techniques. This is required for the interpretation of NMR data in terms of molecular conformation and dynamics. All results are summarized in Table 2.

Table 2. ^{13}C and ^1H Chemical Shift Values (δ) for Doxorubicin in D_2O

| ^{13}C Site* | δ_{C} (ppm) | ^1H Site* | δ_{H} (ppm) |
|-----------------------|---------------------------|--------------------|---------------------------|
| 13 | 214.5 | 2 | 7.48 |
| 5 | 185.6 | 1 | 7.31 |
| 12 | 185.6 | 3 | 7.31 |
| 4 | 160.2 | 1' | 5.34 |
| 11 | 155.5 | 14a | 4.70 |
| 6 | 153.9 | 14b | 4.70 |
| 12a | 133.7 | 7 | 4.64 |
| 2 | 136.6 | 5' | 4.13 |
| 10a | 133.4 | OCH_3 | 3.75 |
| 6a | 133.0 | 4' | 3.74 |
| 3 | 119.5 | 3' | 3.62 |
| 1 | 119.4 | 10ax | 2.80 |
| 4a | 118.5 | 10eq | 2.47 |
| 5a | 110.4 | 8ax | 2.15 |
| 11a | 110.4 | 8eq | 1.91 |
| 1' | 99.8 | 2'ax | 1.90 |

Table 2. ^{13}C and ^1H Chemical Shift Values (δ) for Doxorubicin in D_2O (Continued)

| ^{13}C Site* | δ_{C} (ppm) | ^1H Site* | δ_{H} (ppm) |
|----------------------------|---------------------------|----------------------------|---------------------------|
| 9 | 75.6 | 2'eq | 1.90 |
| 7 | 68.5 | <i>sugar</i> CH_3 | 1.20 |
| 5' | 67.0 | | |
| 4' | 66.2 | | |
| 14 | 64.3 | | |
| OCH_3 | 56.3 | | |
| 3' | 46.6 | | |
| 8 | 35.2 | | |
| 10 | 31.9 | | |
| 2' | 27.5 | | |
| <i>sugar</i> CH_3 | 15.7 | | |

*Numbering schemes for all atomic sites are illustrated in Figure 1.

3.2 NMR Relaxation and Conformational Flexibility

Except in a very few special cases, relaxation times of ^{13}C nuclei in $^{13}\text{CH}_N$ groups ($N>0$) are dominated by dipolar interaction with their directly bonded protons (the ^1H and ^{13}C nuclei are dipolar-coupled). Because the C-H bond length remains constant from molecule to molecule, ^{13}C relaxation times are a reliable probe of molecular mobility. ^{13}C relaxation times are normally measured with full ^1H decoupling to saturate ^1H signals. Under this condition, it is possible to account for NT_1 values of a ^{13}C nucleus in a $^{13}\text{CH}_N$ group with models for explicit molecular motions. ^1H -decoupled T_1 values were measured for 12 protonated carbon atom sites of doxorubicin. Values were measured at a ^{13}C resonance frequency of 125.77 MHz. These values are listed in Table 3 with their corresponding NT_1 values for direct comparison. All T_1 data are accurately described with single-exponential expressions, indicating that ^{13}C relaxation at each of the sites is dominated by a single mechanism. The NT_1 measurements fall between 130-1,400 msec with that for the site on the aromatic ring system (position 2 in Figure 1) significantly shorter than the others. This suggests that relaxation at sites on the aromatic ring system is dominated by molecular tumbling, and relaxation at other sites have additional contributions from conformational motions (rotation about dihedral angles). To a first approximation therefore, the conformational behavior of doxorubicin in solution appears to be a composite of a rigid aromatic ring system, ring librations for the cyclohexane (positions 7, 8, and 10, Figure 1) and carbohydrate rings (positions 2-6), and segmental motions for the pendant $\text{C}(\text{O})\text{CH}_2\text{OH}$ group (position 14).

| Carbon Atom* | T_1 (ms) | NT_1 (ms) |
|-----------------------|------------|-------------|
| 2136 | 136 | |
| 7244 | 244 | |
| 8128 | 256 | |
| 10 | 148 | 296 |
| 14 | 301 | 602 |
| OCH ₃ | 440 | 1,320 |
| 1'250 | 250 | |
| 2'139 | 278 | |
| 3'255 | 255 | |
| 4'298 | 298 | |
| 5'273 | 273 | |
| sugar CH ₃ | 391 | 1,173 |

*Numbering schemes for all atomic sites are illustrated in Figure 1.

3.3 NOESY and trNOESY Analysis

^1H - ^1H NOESY experiments were used to derive interproton distance information for doxorubicin and lavendustin A in solution at 20 °C. Because these ligands are expected to be conformationally flexible under these conditions, the interproton distances are most likely time-weighted average distances. Our relaxation time measurements can be used to unravel the conformational motions giving rise to the time-weighted average distances. The ^1H - ^1H trNOESY experiments, on the other hand, were used to derive interproton distances for both ligands when bound to TetC. Interproton distance information deriving from the trNOESY data reflects the bound conformations of their ligands. TrNOESY is a special case of NOESY used to measure the NOE enhancements for nuclei residing on small molecular ligands when bound to a large macromolecule such as a protein. The ligands must weakly bind the macromolecule so that they remain bound over a very short timeframe. NOE enhancements are destroyed by T_2 relaxation when ligand residence times are long, and enhancements cannot build-up with insufficiently short residence times. The TrNOESY technique relies on the differences in rates of magnetization transfer between protons of a ligand when free in solution and when bound to a macromolecule. Under the appropriate conditions of ligand binding, the relatively faster transfer on the bound ligand can be exploited to measure bound NOE enhancements, reflecting interproton distances for the bound ligand. These are typically positive enhancements and appear in TrNOESY spectra with positive intensities (intensities point upward). In contrast, enhancements between protons on ligands free in solution are almost always negative (intensities point downward), making them easily distinguishable from bound ligand enhancements.

Representative NOESY and trNOESY data are shown in Figure 3, where the same sub-region of the NOESY spectra for doxorubicin (Figure 3A) and lavendustin A (Figure 3B) are compared with the corresponding region of the trNOESY spectrum for the doxorubicin-lavendustin A-TetC complex. A change in sign (positive or negative) for lavendustin A NOE correlation intensities upon TetC binding is evident from a comparison of Figures 3B and 3C.

The lavendustin A NOESY spectrum contains weak negative correlations (Figure 3B, shown in red); however, the addition of TetC results in the same correlations changing their sign (Figure 3C, shown in black), indicating that lavendustin A binds to TetC. Such sign changes were not observed for doxorubicin (Figure 3A), most likely a consequence of the larger doxorubicin molecule's slow tumbling rate prohibiting negative NOE enhancements under the experimental conditions of temperature and magnetic field strength. This is supported by the doxorubicin NOE correlations (D-free in Figure 3A) increasing in intensity upon TetC binding (D-cx in Figure 3C). Moreover, Figure 4 illustrates that the chemical shifts for the doxorubicin NOE intensities (their exact location in the NOESY and trNOESY spectra) change upon TetC binding as well. Collectively, the two figures demonstrate that doxorubicin and lavendustin A bind to TetC, and therefore, tetanus toxin as well at different sites.

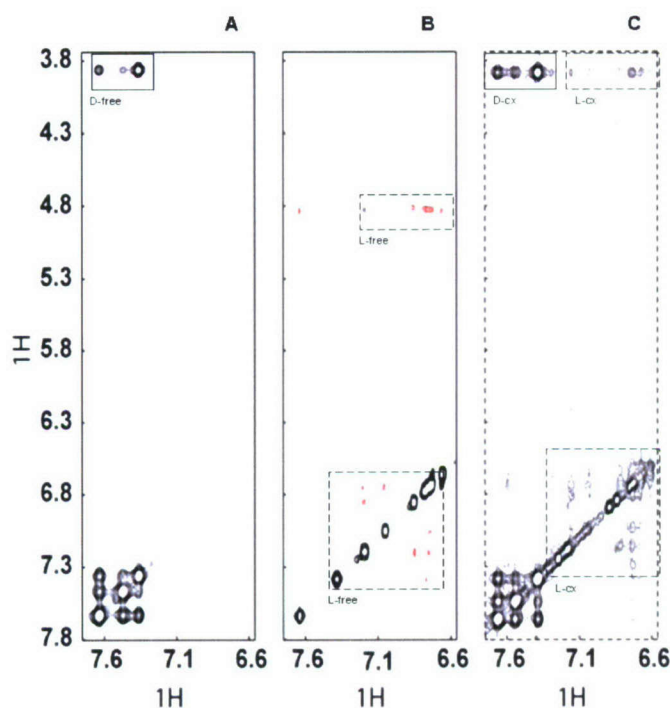


Figure 3. Aromatic Regions of the Doxorubicin (A) and Lavendustin A (B) NOESY Spectra with the Doxorubicin-TetC-lavendustin A Complex trNOESY Spectrum (C). D-free and L-free designate NOE correlations for doxorubicin and lavendustin in solution, respectively, while D-cx and L-cx refer to NOE correlations for these same ligands when bound to TetC.

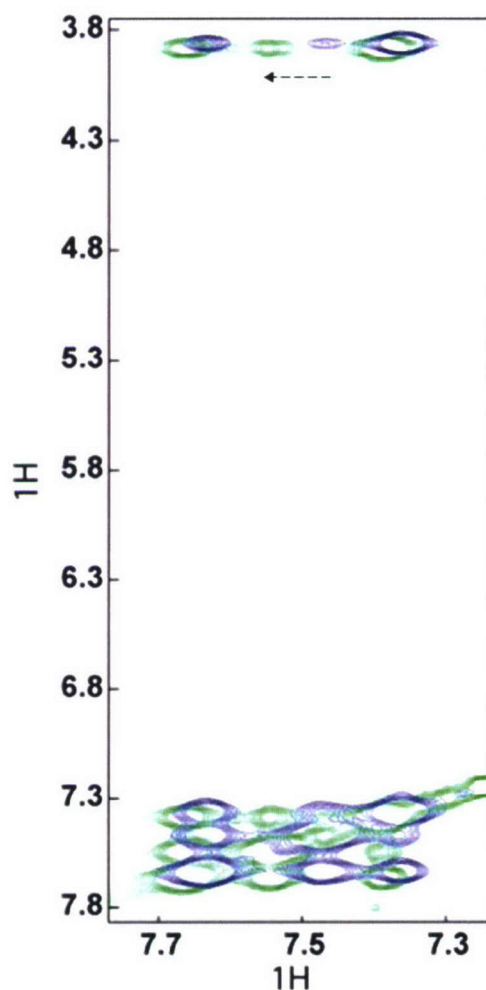


Figure 4. Superposition of the Aromatic Regions from the Doxorubicin NOESY Spectrum (Blue) and trNOESY Spectrum (Green). The arrow indicates the correlations with the largest changes in chemical shift and intensity upon TetC binding.

^1H - ^1H distance constraints were extracted from the NOE correlations shown in Figure 3, as well as those from other trNOESY spectra, to determine the rigid conformations for the ligands when bound to TetC. The binding sites for these ligands were also determined from computer docking experiments with the rigid, TetC bound conformations of the ligands and the TetC molecule (The docking experiments found the orientation and position of the ligand on the TetC fragment with the lowest potential energy). The results of these efforts are summarized in Figures 5 and 6, which are computer-generated images of the doxorubicin and lavendustin A ligands, respectively, bound to TetC. Doxorubicin was found to bind at the same tetanus toxin site as other small ligands, including lactose, which is located in the tetanus toxin β -trefoil folding domain. This is a common surface feature found for the tetanus and botulinum toxins (both are in the family of clostridial neurotoxins). We found the tetanus toxin site for lavendustin A binding to reside on the jelly-roll folding domain, not far from the doxorubicin binding site. Both sites can be described as cavities or pockets in the toxin's surface.

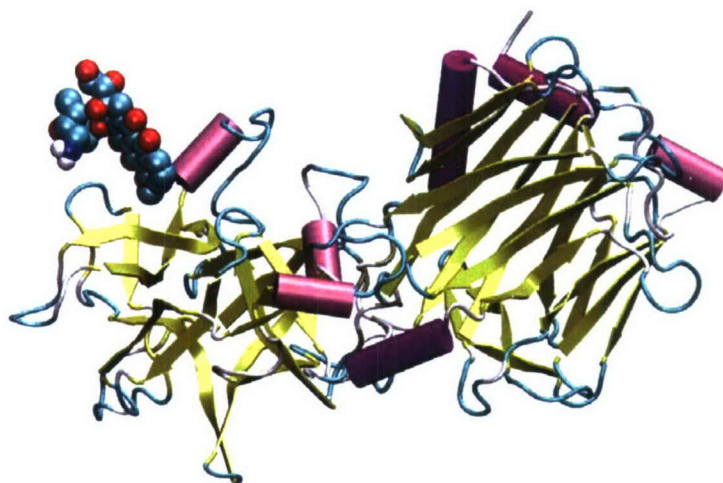


Figure 5. Doxorubicin (Space-filling Model on the Upper Left-hand Corner) Bound to TetC. α -helices are shown as violet cylinders, β -sheets are yellow arrows, and loop regions are blue.

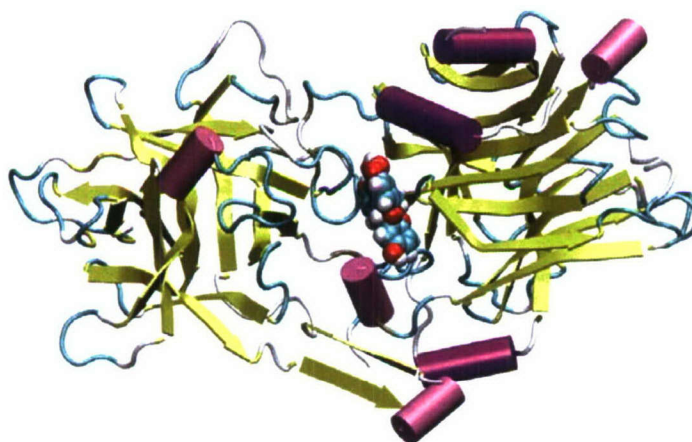


Figure 6. Lavendustin A (Space-filling Model at Center) Bound to the TetC Fragment. See Figure 5 legend for descriptions of TetC features.

4. CONCLUSIONS

Today, there are an ever-increasing number of laboratories investigating the use of small molecules for the design and construction of molecular detectors and biosensors for protein targets. To understand the processes associated with small synthetic ligands binding large protein surfaces, NMR spectroscopy was used to examine the conformational changes in doxorubicin and lavendustin A upon binding to TetC. ^{13}C T_1 measurements suggested that to a first approximation, the conformational behavior of doxorubicin in solution appears to be a

composite of a rigid aromatic ring system, ring librations for its cyclohexane and carbohydrate rings, and segmental motions for the pendant C(O)CH₂OH group. Such conformational flexibility is typical for small molecules and can be expected for both ligands. trNOESY experiments indicated that both ligands adopt rigid conformations when bound to TetC, and as previously demonstrated,^{7,10} each binds a different site on the TetC surface. Experiments are ongoing to measure doxorubicin ¹³C{¹H} spin-spin relaxation times (*T*₂) and steady state NOE enhancements to understand more details of the ligand's conformational flexibility in solution and its contributions to the ligand-TetC binding process.

Blank

LITERATURE CITED

1. Stine, R.; Pishko, V.P.; Schengrund, C.-L. Comparison of Glycosphingolipids and Antibodies as Receptor Molecules for Ricin Detection. *Anal. Chem.* **2005**, *77*, 2882-2888.
2. Fang, Y.; Frutos, A.G.; Lahiri, J. Ganglioside Microarrays for Toxin Detection. *Langmuir* **2003**, *19*, 1500-1505.
3. Laurer, S.; Goldstein, B.; Nolan, R.L.; Nolan, J.P. Analysis of Cholera Toxin-Ganglioside Interactions by Flow Cytometry. *Biochemistry* **2002**, *41*, 1742-1751.
4. Puu, G. An Approach for Analysis of Protein Toxins Based on Thin Films of Lipid Mixtures in an Optical Biosensor. *Anal. Chem.* **2001**, *73*, 72-79.
5. Singh, A.K.; Harrison, S.H.; Schoeniger, J.S. Gangliosides as Receptors for Biological Toxins: Development of Sensitive Fluoroimmunoassays Using Ganglioside-Bearing Liposomes. *Anal. Chem.* **2000**, *72*, 6019-6024.
6. Song, X.; Shi, J.; Swanson, B. Flow Cytometry-Based Biosensor for Detection of Multivalent Proteins. *Anal. Biochem.* **2000**, *284*, 35-41.
7. Cosman, M.; Viswanathan, V. K.; Balhorn, R. Application of NMR Methods to Identify Detection Reagents for Use in Development of Robust Nanosensors. *Methods in Molecular Biology: Protein Nanotechnology, Protocols, Instrumentation, and Applications* (Vo-Dinh, T., ed.) **2005**, *300*, 141-163.
8. Jencks, W.P. What Everyone Wanted to Know About Tight Binding and Enzyme Catalysis, but Never Thought of Asking. *Mol. Biol. Biochem. Biophys.* **1980**, *32*, 3-25.
9. Hajduk, P.J.; Meadows, R.P.; Fesik, S.W. Discovering High-Affinity Ligands for Proteins. *Science* **1997**, *278*, 497-499.
10. Cosman, M.; Lightstone, F.C.; Krishnan, V.V.; Zeller, L.; Prieto, M.C.; Roe, D.C.; Balhorn, R. Identification of Novel Small Molecules that Bind to Two Different Sites on the Surface of Tetanus Toxin C Fragment. *Chem. Res. Toxicol.* **2002**, *15*, 1218-1228.
11. Lightstone, F.C.; Prieto, M.C.; Singh, A.K.; Piqueras, M.C.; Whittal, R.M.; Knapp, M.S.; Balhorn, R.; Roe, D.C. Identification of Small Molecule Ligands that Bind to Tetanus Toxin. *Chem. Res. Toxicol.* **2000**, *13*, 356-362.
12. Searle, M.S.; Maynard, A.J.; Williams, E.L. DNA Recognition by the Anthracycline Antibiotic Respinomycin D: NMR Structure of the Intercalation Complex with d(AGACGTCT)₂. *Royal Soc. Chem.* **2003**, *1*, 60-66.

13. Montecucco, C. Clostridial Neurotoxins. The Molecular Pathogenesis of Tetanus and Botulism. *Current Topics in Microbiology and Immunology* **1995**, 195, Springer-Verlag, Berlin.
14. Winter, A.; Ulrich, W.P.; Wetterich, F.; Weller, U.; Galla, H.J. Gangliosides in Phospholipid Bilayer Membranes: Interaction with Tetanus Toxin. *Chem. Phys. Lipids* **1996**, 81, 21-34.
15. Rogers, T.B.; Snyder, S.H. High Affinity Binding of Tetanus Toxin to Mammalian Brain Membranes. *J. Biol. Chem.* **1981**, 256, 2402-2407.
16. Morris, N.P.; Consiglio, E.; Kohn, L.D.; Habig, W.H.; Hardegree, M.C.; Helting, T.B. Interactions of Fragments B and C of Tetanus Toxin with Neural and Thyroid Membranes and with Gangliosides. *J. Biol. Chem.* **1980**, 255, 6071-6076.
17. Holmgren, J.; Elwing, H.; Fredman, P.; Svennerholm, L. Polystyrene-Adsorbed Gangliosides for Investigation of the Structure of the Tetanus-Toxin Receptor. *Eur. J. Biochem.* **1980**, 106, 371-379.
18. Halpern, J.L.; Loftus, A. Characterization of the Receptor-Binding Domain of Tetanus Toxin. *J. Biol. Chem.* **1993**, 268, 11188-11192.
19. Helting, T.B.; Zwisher, O. Structure of Tetanus Toxin. I. Breakdown of the Toxin Molecule and Discrimination between Polypeptide Fragments. *J. Biol. Chem.* **1977**, 252, 187-193.
20. Shapiro, R.E.; Specht, C.D.; Collins, B.E.; Woods, A.S.; Cotter, R.J.; Schnaar, R.L. Identification of a Ganglioside Recognition Domain of Tetanus Toxin Using a Novel Ganglioside Photoaffinity Ligand. *J. Biol. Chem.* **1997**, 272, 30380-30386.
21. Emsley, P.; Fotinou, C.; Black, I.; Fairweather, N.F.; Charles, I.G.; Watts, C.; Hewitt, E.; Isaacs, N.W. The Structures of the H(C) Fragment of Tetanus Toxin with Carbohydrate Subunit Complexes Provide Insight into Ganglioside Binding. *J. Biol. Chem.* **2000**, 275, 8889-8894.
22. Eswaramoorthy, S.; Kumaran, D.; Swaminathan, S. Crystallographic Evidence for Doxorubicin Binding to the Receptor Binding Site in *Clostridium botulinum* neurotoxin B. *Acta Crystallogr.* **2001**, 57, 1743-1746.
23. Ginalski, K.; Venclovas, C.; Lesyng, B.; Fidelis, K. Structure-Based Sequence Alignment for the β -Trefoil Subdomain of the *Clostridium* Neurotoxin Family Provides Residue Level Information about the Putative Ganglioside Binding Site. *FEBS Lett.* **2000**, 482, 119-124.

24. Kraus-Berthier, L.; Jan, M.; Guildbaud, N.; Naze, M.; Pierre, A.; Atassi, G. Histology and Sensitivity to Anticancer Drugs of Two Human Nonsmall Cell Lung Carcinomas Implanted in the Pleural Cavity of Nude Mice. *Clin. Cancer Res.* **2000**, *6*, 297-304.
25. Friesen, C.; Fulda, S.; Debatin, K.M. Cytotoxic Drugs and the CD95 Pathway. *Leukemia* **1999**, *13*, 1854-1858.
26. Sparano, J.A. Doxorubicin/Taxane Combinations: Cardiac Toxicity and Pharmacokinetics. *Semin. Oncol.* **1999**, *26*, 14-19.
27. Onoda, T.; Iinuma, H.; Sasaki, Y.; Hamada, M.; Isshiki, K.; Naganawa, H.; Takeuchi, T.; Tatsuta, K.; Umezawa, K. Isolation of a Novel Tyrosine Kinase Inhibitor, Lavendustin A, from *Streptomyces griseolavendus*. *J. Nat. Prod.* **1989**, *52*, 1252-1257.
28. Shaka, A.J.; Keeler, J.; Freeman, R. Evaluation of a New Broadband Decoupling Sequence: WALTZ-16. *J. Magn. Reson.* **1983**, *53*, 313-340.
29. Henderson, T.J. Sensitivity-Enhanced Quantitative ^{13}C NMR Spectroscopy via Cancellation of 1JCH Dependence in DEPT Polarization Transfers. *J. Am. Chem. Soc.* **2004**, *126*, 3682-3683.
30. Farrar, T.C.; Becker, E.D. *Pulse and Fourier Transform NMR*; Academic Press: New York, 1967; pp 278-286.
31. Redfield, A.G.; Kunz, S.D. Quadrature Fourier NMR Detection: Simple Multiplex for Dual Detection and Discussion. *J. Magn. Reson.* **1975**, *19*, 250-254.
32. Palmer III, A.G.; Cavanaugh, J.; Wright, P.E.; Rance, M. Sensitivity Improvement in Proton-Detected Two-Dimensional Heteronuclear Correlation NMR Spectroscopy. *J. Magn. Reson.* **1991**, *93*, 151-170.
33. Kay, L.E.; Keifer, P.; Saarinen, T. Pure Absorption Gradient Enhanced Heteronuclear Single Quantum Correlation Spectroscopy with Improved Sensitivity. *J. Am. Chem. Soc.* **1992**, *114*, 10663-10665.
34. Schleucher, J.; Schwendinger, M.; Sattler, M.; Schmidt, P.; Schedletzky, O.; Glazer, S.J.; Sorensen, O.W.; Griesinger, C. A General Enhancement Scheme in Heteronuclear Multidimensional NMR Employing Pulsed Field Gradients. *J. Biomol. NMR* **1994**, *4*, 301-306.
35. Wagner, R.; Berger, S. Gradient-Selected NOESY - a Fourfold Reduction of the Measurement Time for the NOESY Experiment. *J. Magn. Reson. Series A* **1996**, *123*, 119-121.
36. States, D.J.; Haberkorn, R.A.; Ruben, D.J. A Two-Dimensional Nuclear Overhauser Experiment with Pure Absorption Phase in Four Quadrants. *J. Magn. Reson.* **1982**, *48*, 286-292.

37. Noggle, J.; Schirmer, R. *The Nuclear Overhauser Effect: Chemical Applications*; Academic Press: New York, 1971.
38. Olejniczak, E.; Eaton, H. Extrapolation of Time Domain Data with Linear Prediction Increases Resolution in Both Dimensions. *J. Magn. Reson.* **1990**, 87, 628-632.